Supporting information

Efficient homogeneous electrochemical water oxidation by a copper(II) complex of hexaaza macrotricyclic ligand

Junqi Lin,[a*]‡ Shenke Zheng,[a]‡ Li Hong,[a] Xueli Yang,[a] Weixiang Lv,[b] Yichang Li,[b] Chang Dai,[a] Shanshan Liu,[*] Zhijun Ruan[*a]

[a] Hubei Key Laboratory of Processing and Application of Catalytic Materials, College of Chemistry and Chemical Engineering, Huanggang Normal University, Huanggang, 438000 China

[b] Weifang Synovtech New Material Technology CO., LTD, Weifang, Shandong Province, 262700, P.R. China

* To whom correspondence should be addressed.

E-mail addresses: linjunqi@hgnu.edu.cn, cingym@126.com, ruanzhijun@hgnu.edu.cn

Table S1 Crystal data and structure refinement for complex **1**.

Identification code	T	
Empirical formula	C24 H52 Cl4 Cu2 N12 O16	
Formula weight	1033.62	
Temperature	293(2) K	
Wavelength	0.710 73 Å	
Crystal system	Triclinic	
Space group	P-1	
Unit cell dimensions	a = 8.5097(4) Å	a= 73.650(2)°.
	b = 8.5847(4) Å	b= 80.262(2)°.
	c = 15.1931(8) Å	g = 69.8330(10)°.
Volume	996.52(9) $Å^3$	
Z	1	
Density (calculated)	1.716 Mg/m^3	
Absorption coefficient	1.418 mm^{-1}	
F(000)	530	
Crystal size	0.260 x 0.250 x 0.240 mm^3	
Theta range for data collection	2.558 to 25.997°.	
Index ranges	-10<=h<=10, -10<=k<=10, -18<=l<=18	
Reflections collected	31794	
Independent reflections	3896 [R(int) = 0.0717]	
Completeness to theta = 25.242°	99.6 %	
Absorption correction	Semi-empirical from equivalents	
Max. and min. transmission	0.7457 and 0.6884	
Refinement method	Full-matrix least-squares on F^2	
Data / restraints / parameters	3896 / 0 / 265	
Goodness-of-fit on F^2	1.054	
Final R indices [I>2sigma(I)]	R1 = 0.0740, wR2 = 0.2097	
R indices (all data)	R1 = 0.0928, wR2 = 0.2277	
Extinction coefficient	n/a	
Largest diff. peak and hole	1.779 and -0.608 e.$Å^{-3}$	

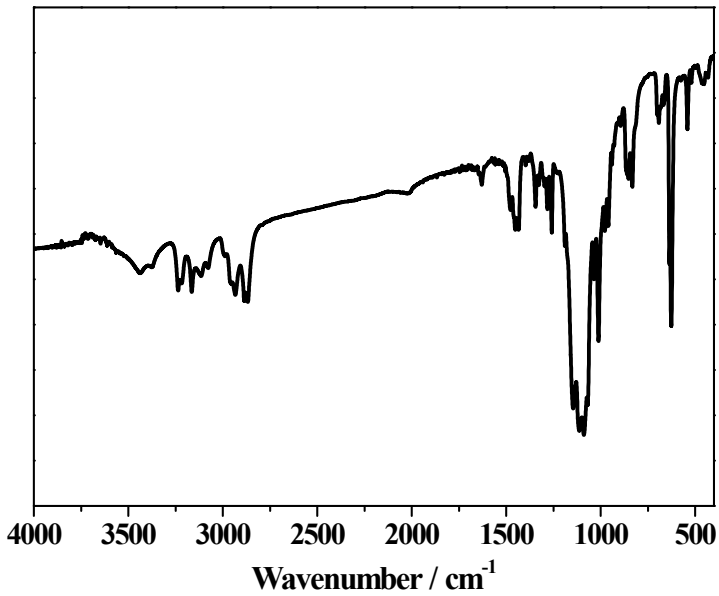

Fig. S1 FTIR spectrum of $[Cu^{II}(L)](ClO_4)_2$.

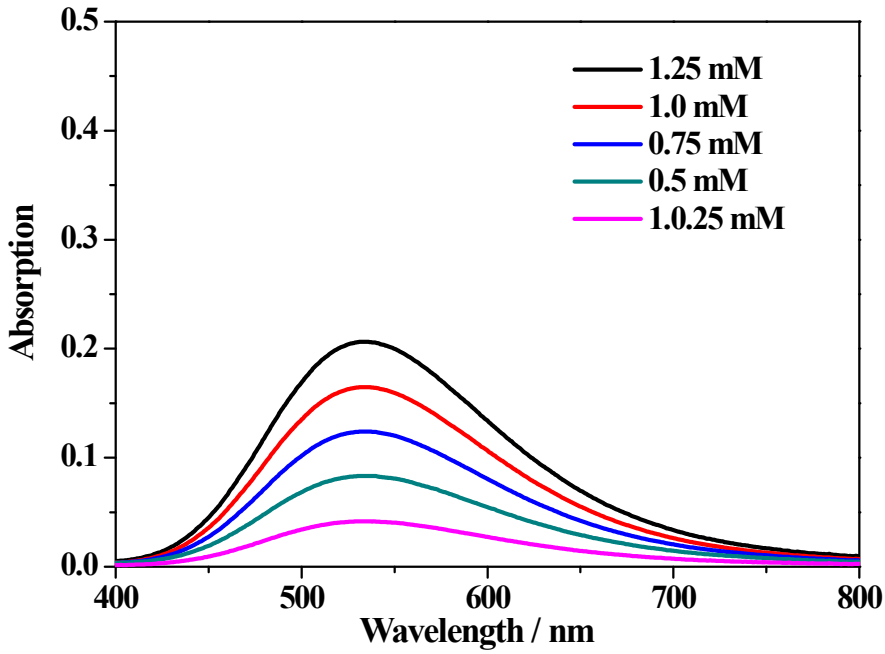

Fig. S2 UV-Vis absorption of $[Cu^{II}(L)](ClO_4)_2$ at different concentrations in neutral phosphate buffer solution.

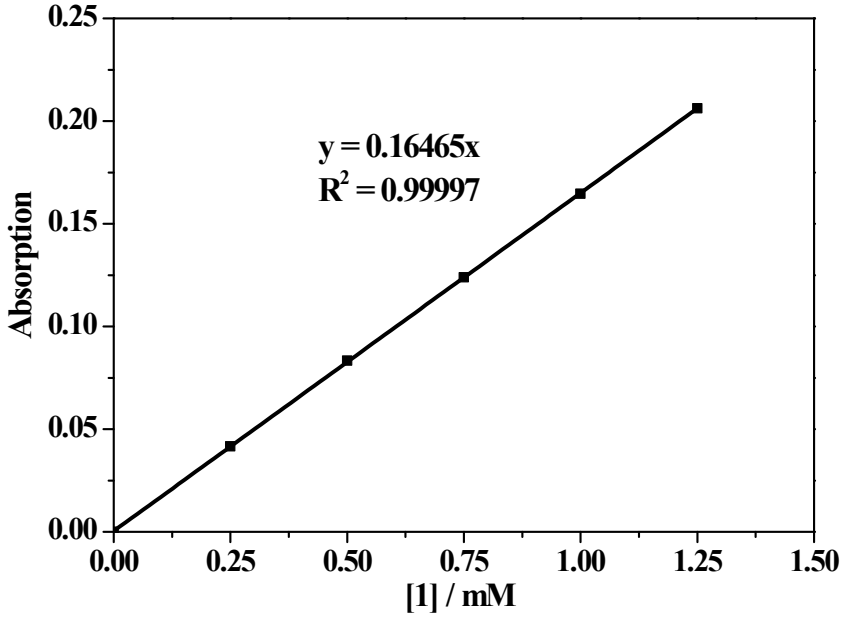

Fig. S3 Linear relationship between the UV-Vis absorption at 532 nm and the concentration of $[Cu^{II}(L)](ClO_4)_2$.

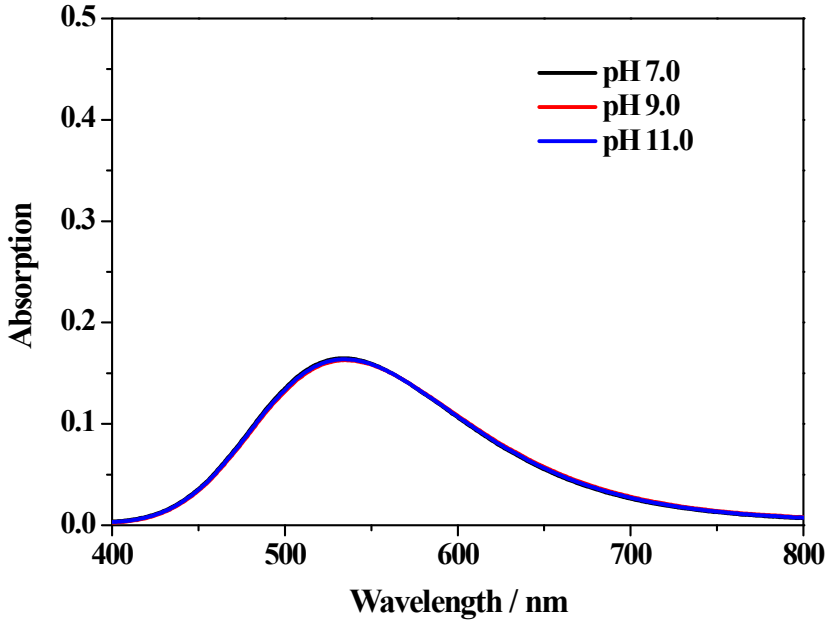

Fig. S4 UV-Vis absorption spectra of $[Cu^{II}(L)](ClO_4)_2$ in PBS at various pH.

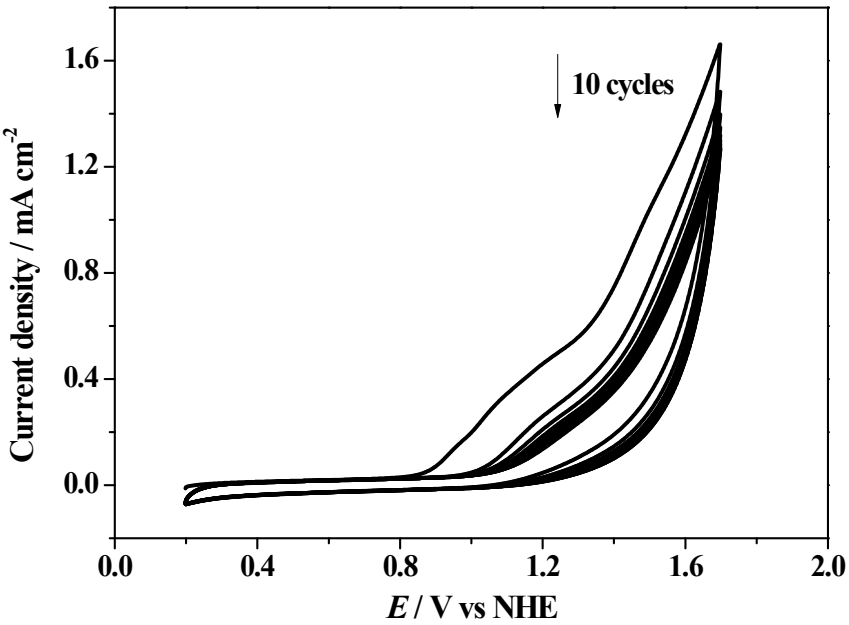

Fig. S5 Continuous CV scans of 10 times over $[Cu^{II}(L)](ClO_4)_2$ in phosphate-buffered solution at pH 7.0; GC electrode (0.071 cm^2) was used as working electrode and scan rate was 100 mV/s.

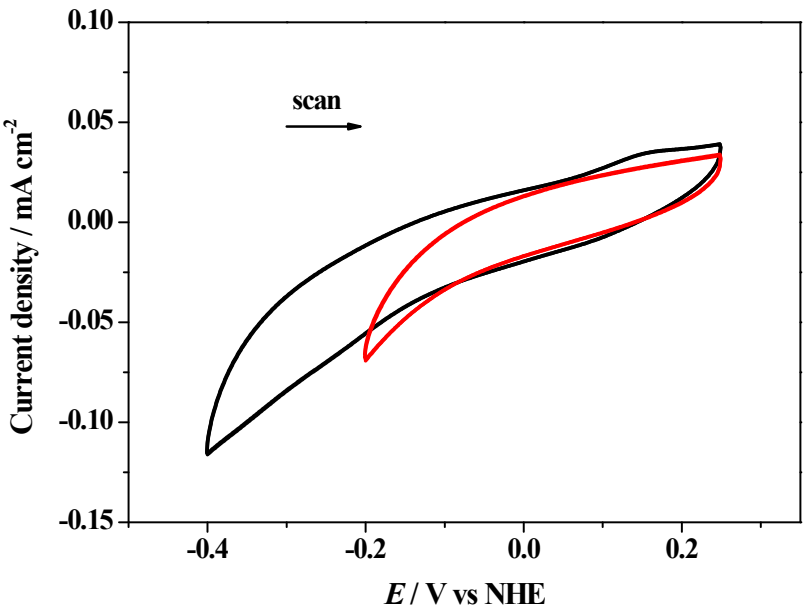

Fig. S6 CV scan of 1 mM $[Cu^{II}(L)](ClO_4)_2$ in phosphate-buffered solution at pH 7.0; GC electrode (0.071 cm^2) was used as working electrode and scan rate was 100 mV/s.

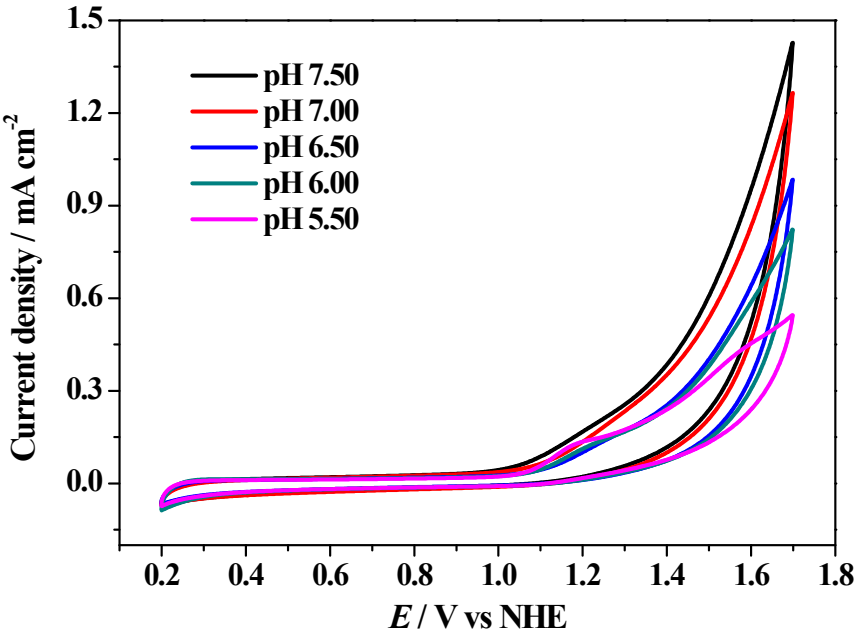

Fig. S7 CV scans of $[Cu^{II}(L)](ClO_4)_2$ in phosphate-buffered solution at different pH values. GC electrode (0.071 cm^2) was used as working electrode and scan rate was 100 mV/s.

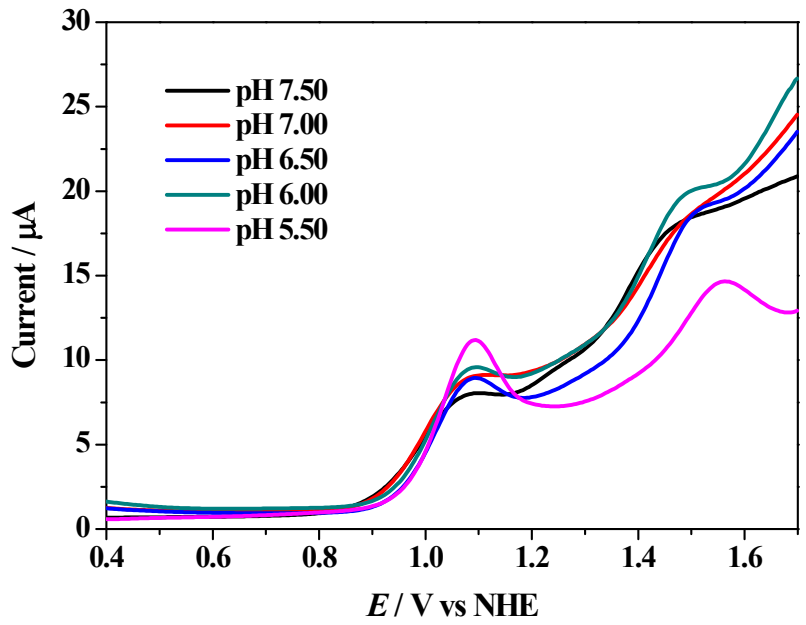

Fig. S8 DPVs of 1 mM **1** in 0.1 M PBS at different pH values. DPVs were obtained with parameters: amplitude = 50 mV, step height = 4 mV, pulse width = 0.05 s, pulse period = 0.5 s and sampling width = 0.0167 s.

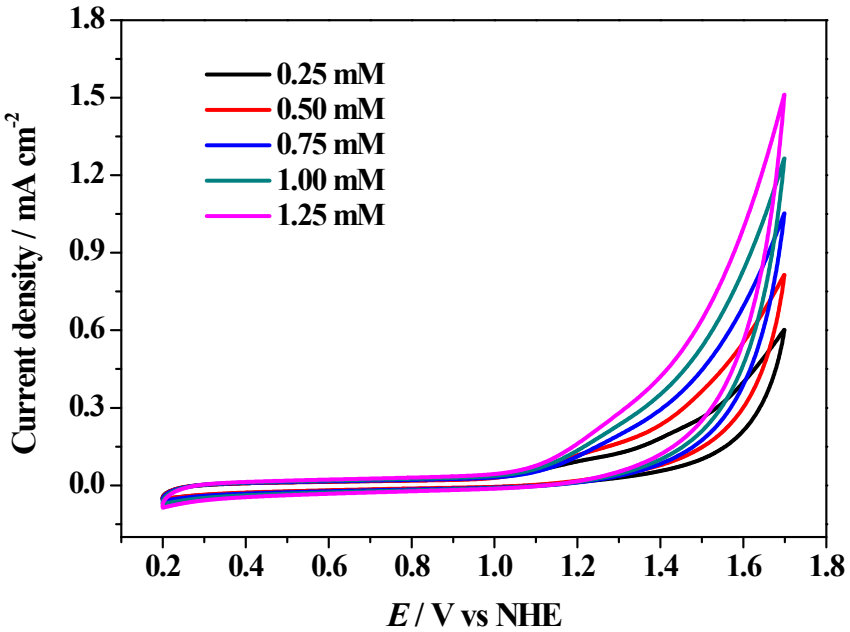

Fig. S9 CV scans of $[Cu^{II}(L)](ClO_4)_2$ at different concentrations in phosphate-buffered solution at pH 7.0; GC electrode (0.071 cm^2) was used as working electrode and scan rate was 100 mV/s.

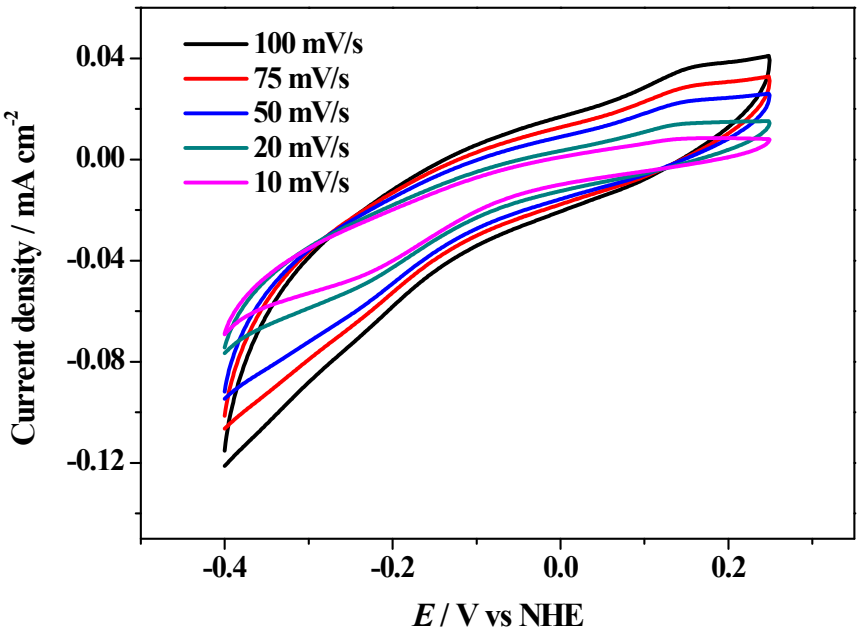

Fig. S10 CV scans of 1 mM $[Cu^{II}(L)](ClO_4)_2$ in phosphate-buffered solution at pH 7.0 with different scan rates between -0.4 V and 0.25 V vs NHE; GC electrode (0.071 cm^2) was used as working electrode.

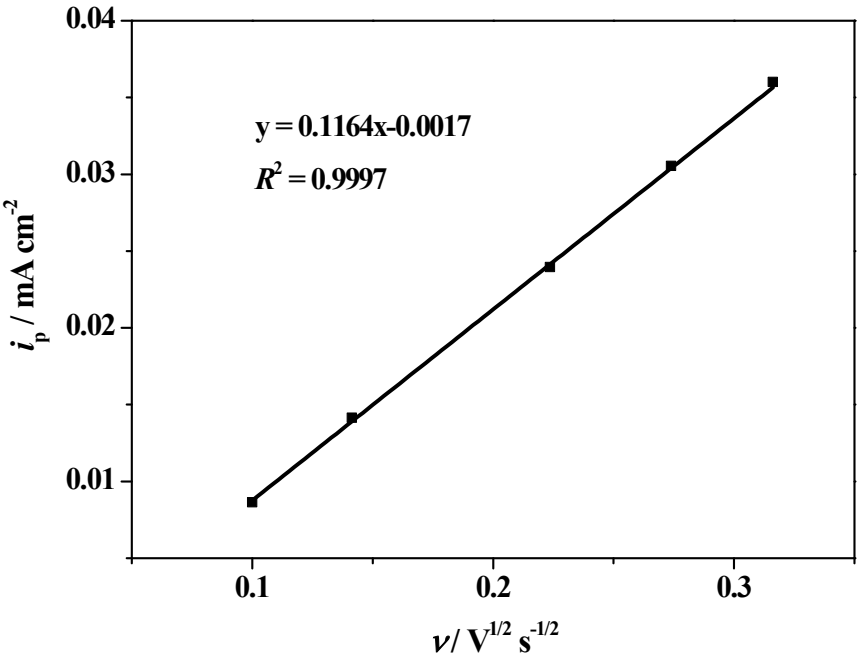

Fig. S11 Scan rate dependence of peak current i_p (the maximal current of the oxidative wave) in the case of 1 mM of **1** in 0.1 M phosphate-buffered solution.

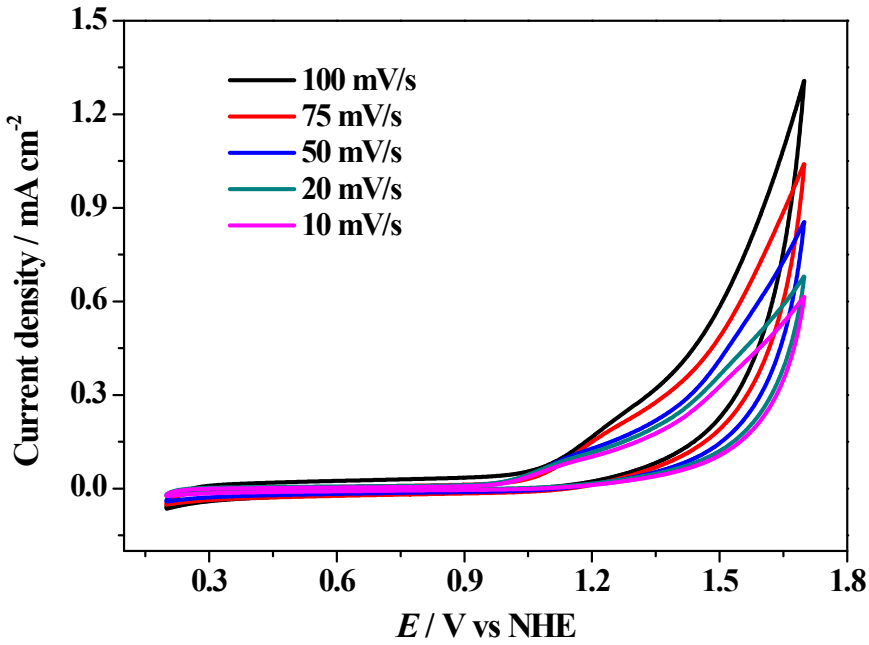

Fig. S12 CV scans of 1 mM $[Cu^{II}(L)](ClO_4)_2$ in phosphate-buffered solution of pH 7.0 at different scan rates; GC electrode (0.071 cm^2) was used as working electrode.

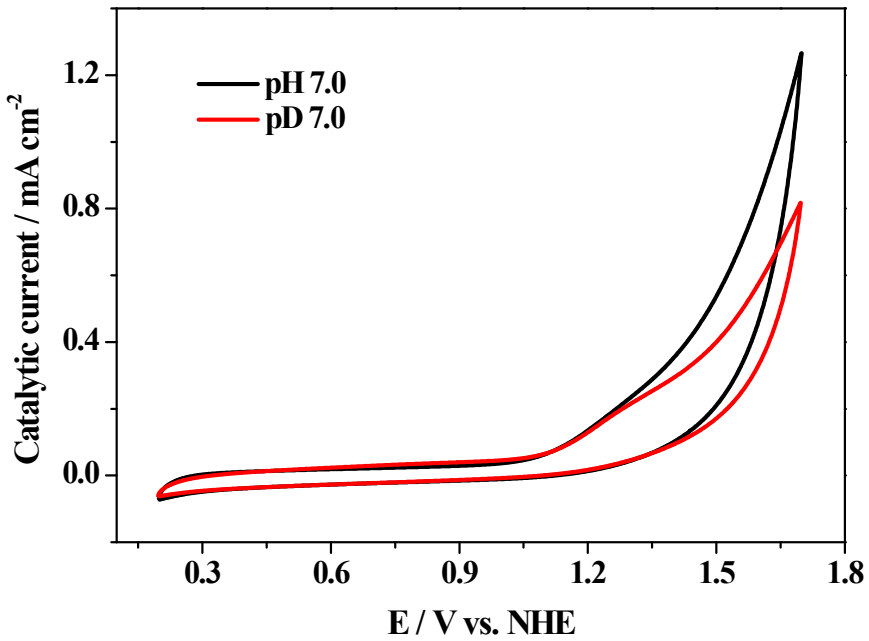

Fig. S13 CV tests of 1 mM of $[Cu(L)](ClO_4)_2$ in phosphate buffer solution at pH 7.0 and pD 7.0.

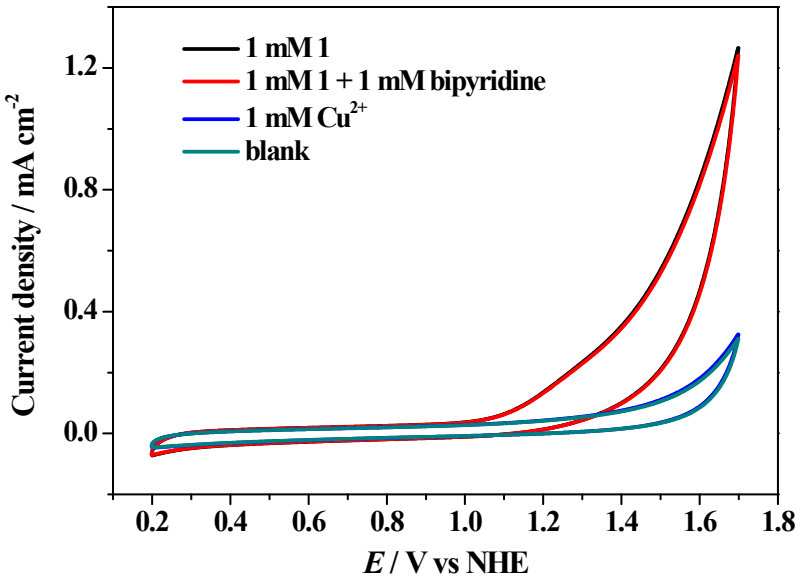

Fig. S14 CV scan of 1 mM Cu^{2+} (blue), 1.0 mM **1** in the absence (balck) and presence (red) of 1.0 mM bipyridine; GC electrode was used as working electrode and scan rate was 100 mV/s.

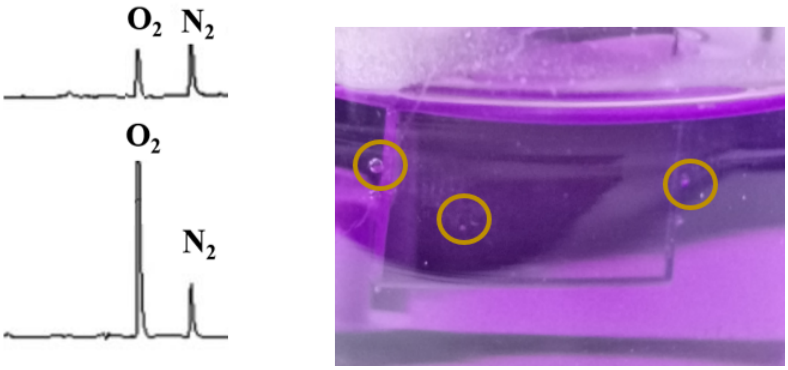

Fig. S15 The gas chromatography diagram of the evolved oxygen (left) and the photograph of the oxygen bubbles generated during CPE test (right).

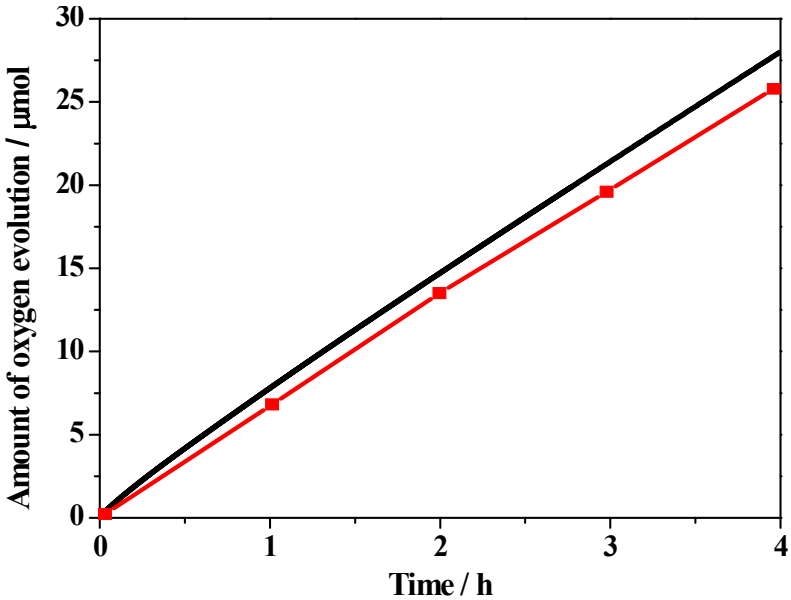

Fig. S16 Faradaic efficiency of O_2 evolution for **1** in 0.1 M PBS of pH 7.0 at 1.6 V vs NHE in 4 h of electrolysis. The red line represents the amount of evolved O_2 quantified by GC analysis. The black line represents the amount of O_2 expected for a 100% faraday efficiency according to the total charge that passed during 4 h of electrolysis.

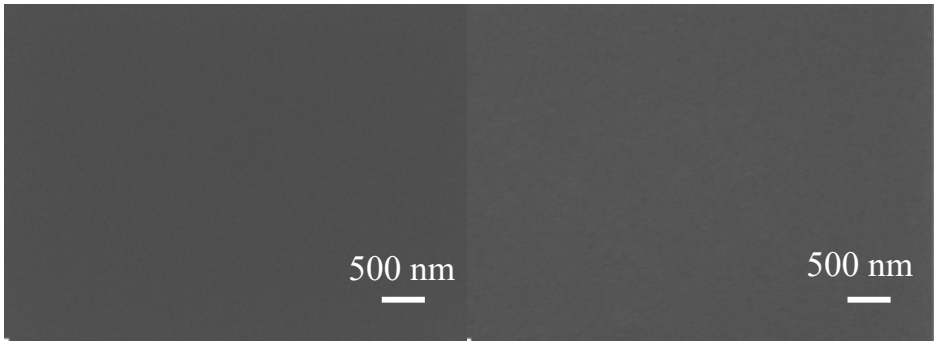

Fig. S17 SEM images of the surface of ITO electrode before (left) and after (right) 4 h of CPE experiments of **1** in 0.1 M phosphate buffer solution at neutral pH.

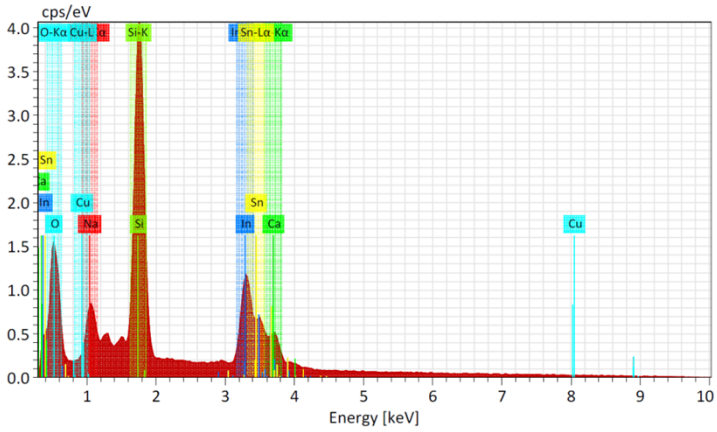

Fig. S18 EDX analysis of the ITO electrode before CPE test.

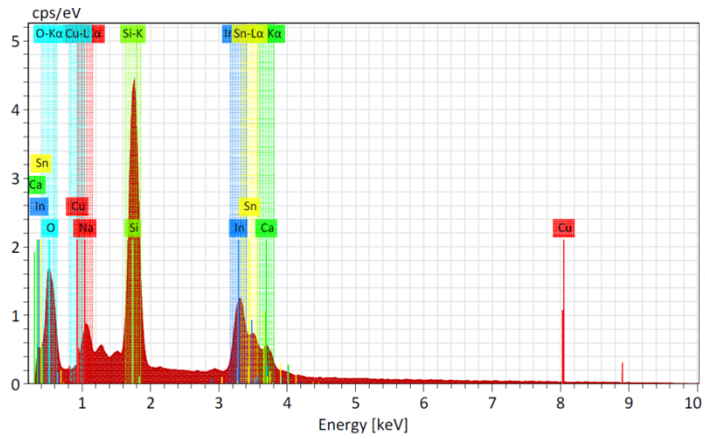

Fig. S19 EDX analysis of the ITO electrode after CPE test.

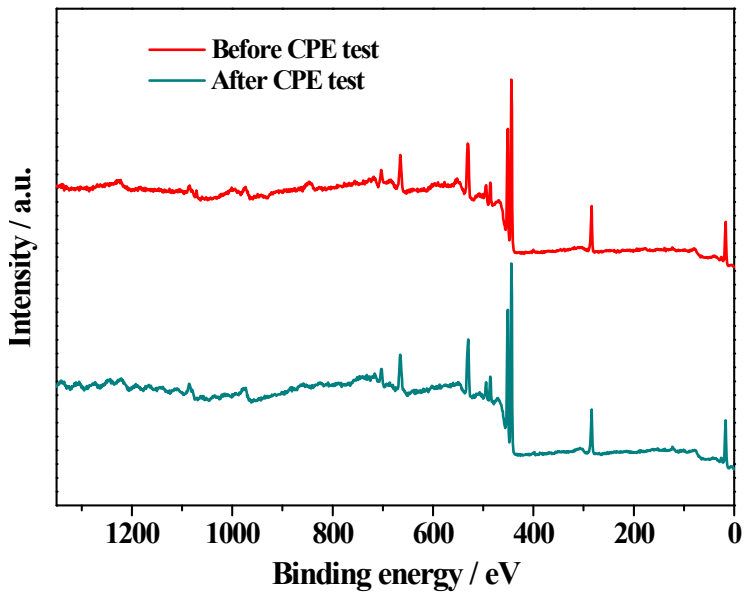

Fig. S20 Full scan of XPS spectra of ITO electrode before and after CPE test with complex 1 as catalyst.

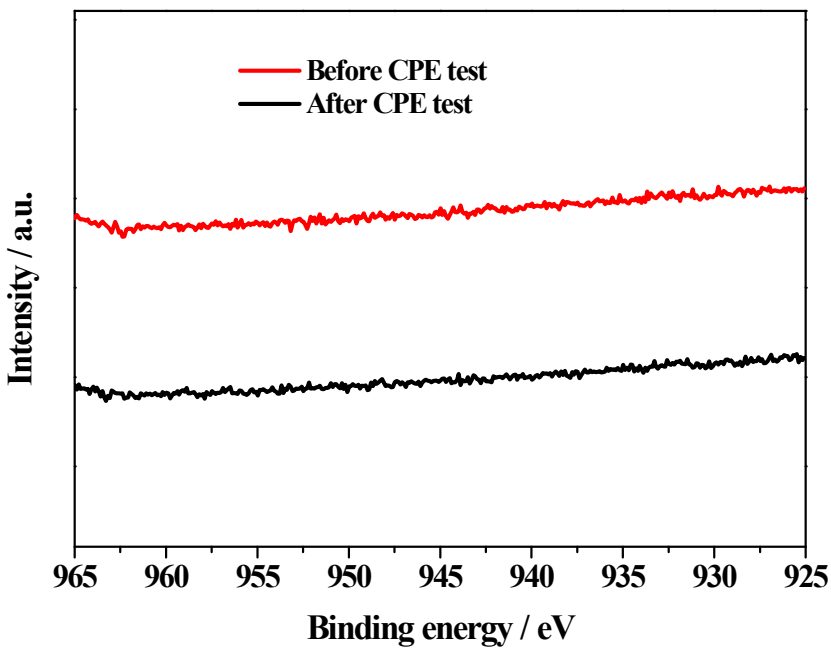

Fig. S21 XPS spectra of Cu element on ITO electrode before and after CPE test with complex **1** as catalyst.

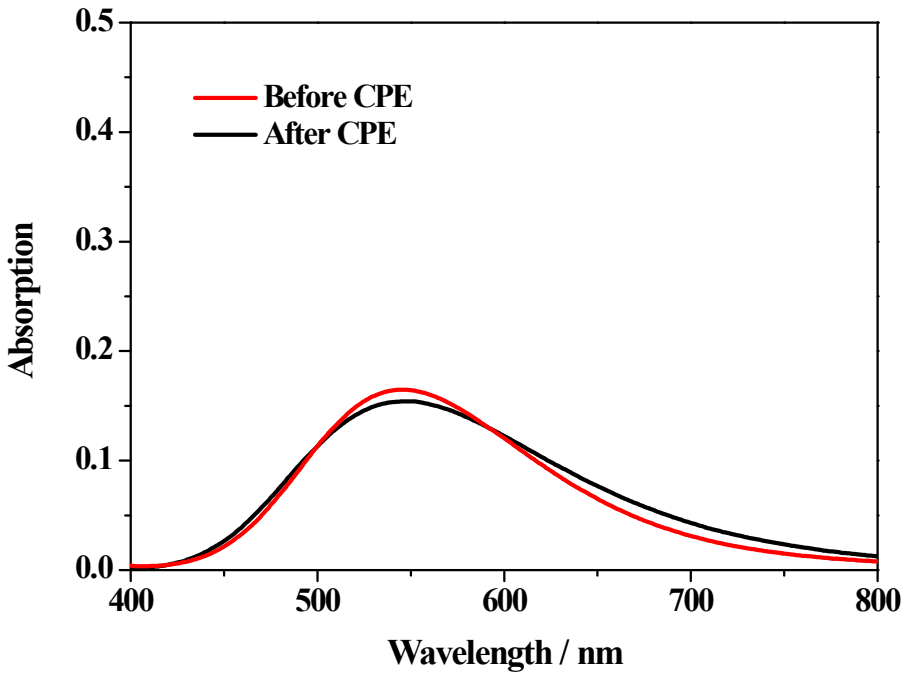

Fig. S22 UV-Vis absorption spectra of 1 mM of **1** before and after 4 h of CPE test.

Table S2 Overpotential and kinetic date of homogeneous electrochemical water oxidation catalyzed by Cu-based complex

Catalyst [a]	pH	η/mV [b]	Potential/V [c]	TOF	TON	FE/%	Ref.
$[Cu(I)(C2)]^{+}$	6.5	674	1.73	9.77	4.6	/	S1
$[Cu(en)_2(OH_2)_2]^{2+}$	8.0	440	1.55	0.4	/	75	S2
$[Cu(H_2L)(OH)_2]$	12.4	640	1.24	0.4	~1	85	S3
$[(L2)Cu]^{2-}$	11.5	400	0.95	3.58	/	/	S4
$[Cu(H_2L)]^{2+}$	7.0	580	1.60	11.09	/	95	S5
$[L\text{-}Cu\text{-}CO_3H]^{-}$	10.0	650	1.60	20.1	3.91	95	S6
$[Cu^{II}(L)]^{2+}$	12.9	830	1.35	0.12	6	60	S7
$[(L4)Cu]^{2-}$	11.6	754	1.39	9.77	1.86	76	S8
$[Cu_2(TPMAN)(\mu\text{-}OH)(H_2O)]^{3+}$	7.0	780	1.87	0.78	/	/	S9
$[Cu(pyalk)_2]$	12.5	550	1.13	0.7	30	75	S10
$[CuL_2]^{2+}$	9.20	602	1.50	11.84	/	86	S11
$[Cu(N_2Py_3)]^{2+}$	11.0	831	1.60	0.81	/	/	S12
$[(DAM)Cu_3(\mu^3\text{-}O)]^{4+}$	7.0	550	1.62	19.1	/	45 [d]	S13
$[Cu(TMC)(OH_2)]^{2+}$	7.0	580	1.77	30	362	89	S14
Cucyclam	7.0	880	/	/	/	/	S15
$CuMe_4$cyclam	7.0	880	1.75	7	/	88	S15
$[CuL(OH_2)]^{2+}$	12.0	530	/	/	4	50	S16
Complex **1**	7.0	480	1.48	3.65	1.04	90	This work

[a] The structures of the catalysts listed in this table are given below. [b] η = onset overpotential obtained from CV test (vs. NHE). [c] Potential used for the calculation of k_{cat}. [d] Measure at pH 8.1.

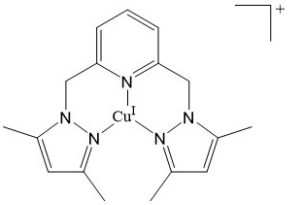

$[Cu(I)(C2)]^{+}$

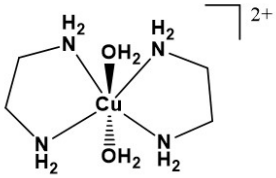

$[Cu(en)_2(OH_2)_2]^{2+}$

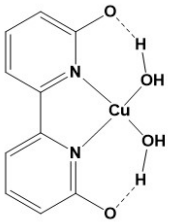

$[Cu(H_2L)(OH)_2]$

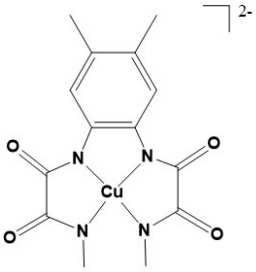

$[(L2)Cu]^{2-}$

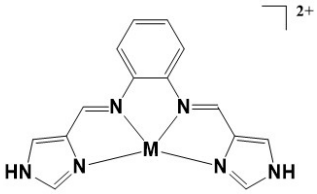

$[Cu(H_2L)]^{2+}$

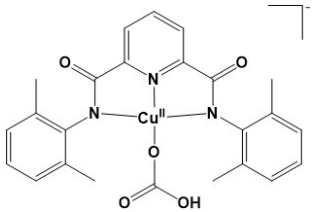

$[L\text{-}Cu\text{-}CO_3H]^{-}$

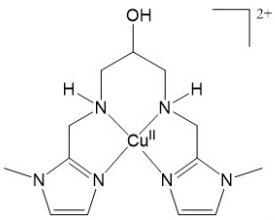

$[Cu^{II}(L)]^{2+}$

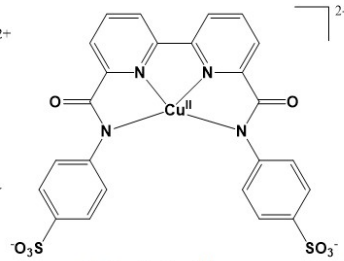

$[(L4)Cu]^{2-}$

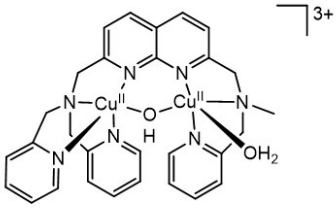

$[Cu_2(TPMAN)(\mu\text{-}OH)(H_2O)]^{3+}$

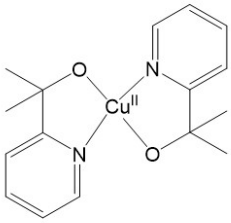

$[Cu(pyalk)_2]$

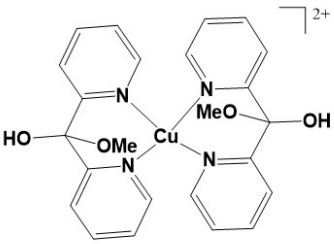

$[CuL_2]^{2+}$

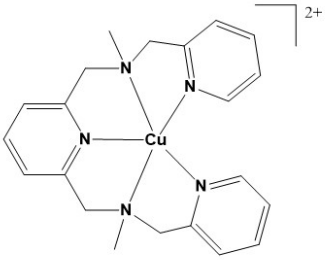

$[Cu(N_2Py_3)]^{2+}$

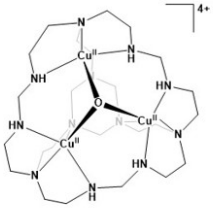

$[(DAM)Cu_3(\mu^3\text{-}O)]^{4+}$

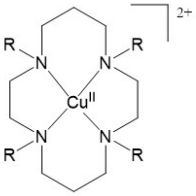

R = H Cucyclam
R = H $CuMe_4$cyclam

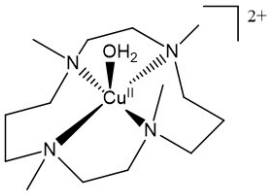

$[Cu(TMC)(OH_2)]^{2+}$

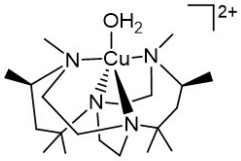

$[CuL(OH_2)]^{2+}$

Reference

[1] T. Makhado, B. Das, R. J. Kriek, H. C. M. Voslooa and A. J. Swarts. *Sustainable Energy Fuels*, 2021, **5**, 2771–2780.

[2] C. Lu, J. Du, X. J. Su, M. T. Zhang, X. Xu, T. J. Meyer and Z. Chen. *ACS Catal.*, 2016, **6**, 77–83.

[3] T. Zhang, C. Wang, S. Liu, J. L. Wang and W. Lin, *J. Am. Chem. Soc.*, 2014, **136**, 273–281.

[4] P. Garrido-Barros, I. Funes-Ardoiz, S. Drouet, J. Benet-Buchholz, F. Maseras and A. Llobet, *J. Am. Chem. Soc.*, 2015, **137**, 6758–6761.

[5] J. Lin, X. Chen, N. Wang; S. Liu, Z. Ruan and Y. Chen. *Catal. Sci. Technol.*, 2021, **11**, 6470–6476.

[6] F. Chen, N. Wang, H. Lei, D. Guo, H. Liu, Z. Zhang, W. Zhang, W. Lai and R. Cao. *Inorg. Chem.*, 2017, **56**, 13368–13375.

[7] S. Nestke, E. Ronge and I. Siewert. *Dalton Trans.*, 2018, **47**, 10737–10741.

[8] M. Gil-Sepulcre, P. Garrido-Barros, J. Oldengott, I. Funes-Ardoiz, R. Bofill, X. Sala, J. Benet-Buchholz and A. Llobet. *Angew. Chem. Int. Ed.*, 2021, **60**, 18639–18644.

[9] Q.-Q. Hu, X.-J. Su and M.-T. Zhang, *Inorg. Chem.*, 2018, **57**, 10481–10484

[10] K. J. Fisher, K. L. Materna, B. Q. Mercado, R. H. Crabtree and G. W. Brudvig, *ACS Catal.*, 2017, **7**, 3384–3387.

[11] N. N. Shi , W. J. Xie , D. M. Zhang, Y. H. Fan, L. S. Cui and M. Wang. *J. Electroanal. Chem.*, 2021, **886**, 115106.

[12] Z. Xu, Z. Zheng, Q. Chen, J. Wang, K. Yu, X. Xia, J. Shen and Q. Zhang, *Dalton Trans*. 2021, **50**, 10888–10895.

[13] A. M. Geer, C. Musgrave III, C. Webber, R. J. Nielsen, B. A. McKeown, C. Liu, P. P. M. Schleker, P. Jakes, X. Jia, D. A. Dickie, J. Granwehr, S. Zhang, C.W. Machan, W. A. Goddard and T. Brent Gunnoe, *ACS Catal.*, 2021, **11**, 7223–7240.

[14] F. Yu, F. Li, J. Hu, L. Bai, Y. Zhu and L. Sun, *Chem. Commun.*, 2016, **52**, 10377−10380.

[15] A. Prevedello, I. Bazzan, N. D. Carbonare, A. Giuliani, S. Bhardwaj, C. Africh, C. Cepek, R. Argazzi, M. Bonchio, S. Caramori, M. Robert and A. Sartorel, *Chem. Asian J.*, 2016, **11**, 1281−1287.

[16] J. Wang, H. Huang and T. Lu, *Chin. J. Chem.*, 2017, **35**, 586–590.